Electronic Supporting Information (ESI)

ZnO Quantum Dots as an Electron-Transport Layer for Highly Efficient and Stable Organic Solar Cells

Abdus Saboor[1,2], Oleksandr Stroyuk[2*], Oleksandra Raievska[2], Chao Liu[2*], Jens Hauch[1,2], Christoph J. Brabec[1,2]

[1]*Friedrich-Alexander-Universität Erlangen-Nürnberg, Materials for Electronics and Energy Technology (i-MEET), Martensstrasse 7, 91058 Erlangen, Germany*
[2]*Forschungszentrum Jülich GmbH, Helmholtz-Institut Erlangen Nürnberg für Erneuerbare Energien (HI ERN), 91058 Erlangen, Germany*

Materials and Methods

Materials. PM6, L8BO, $PC_{70}BM$, and BTP-eC9 absorbers were purchased from Solarmer, Solenne BV. Reference colloidal zinc oxide (Product N-10, 2.5 w.% ZnO in 2-propanol) was received from Avantama and used as supplied. Hole transport material ink BM-HTL-1 was supplied by Brilliant Matters.

Zinc acetate dihydrate, NaOH, dry ethanol, hexane, dimethyl sulfoxide, toluene, chloroform, and o-xylene were purchased from Sigma-Aldrich and used as received.

Optimized synthesis of ZnO QD ink. Colloidal ZnO QDs were produced at room temperature in a reaction between two precursors. Precursor #1 was prepared by dissolving 3.0 mmol (0.658 g) of $ZnAc_2 \times 2H_2O$ (Ac is acetate)in 7 mL of dry dimethyl sulfoxide (DMSO) under intense stirring, then an additional amount of DMSO was added to reach a volume of 7.5 mL. The final solution contains 0.4 M $ZnAc_2$ with traces of water stemming from the crystal hydrate.

For Precursor #2, a 10 M NaOH solution in water was prepared by dissolving 2.0 g NaOH in 5.0 mL deionized (DI) water. Then, 70 μL of NaOH solution was added at intense stirring to 2.5 mL of dry ethanol (EtOH, 99%). Only freshly prepared Precursor #2 was used for the synthesis, while the storage resulted in the EtOH evaporation and the crystallization of NaOH on the surface of the solution.

For the synthesis of ZnO QDs, 1.25 mL of Precursor #1 is introduced into a glass vial (5 mL), and the entire volume of freshly prepared Precursor #2 is added with intense magnetic stirring. The mixing is performed at room temperature (RT). The vial is closed with a cap after the precursor mixing to prevent ambient water vapor adsorption by dry EtOH and to avoid solvent evaporation, and left under magnetic stirring for an additional 5 min at RT. The mixing of the precursors results in the formation of a non-transparent suspension, followed by the complete dissolution of the precipitate after 1-2 min of magnetic stirring and the formation of a transparent solution.

The vial with the transparent solution is transferred into a heating unit (a Fischer block with 1 cm wells for vials) pre-heated to 60 ^{o}C and kept at this temperature for 10 min under a closed cap. With the heating complete, the vial is left to cool to RT for 5 min, and the solution is transferred into a plastic centrifugation 15-mL vial. Then, 4.0 mL of an antisolvent mixture (2:1 v/v hexane/toluene) is added to the plastic vial, followed by centrifugation at 5000 rpm for 5 min.

After centrifugation, the supernatant is separated and discarded, and 1.5 mL of dry (99%) EtOH containing 15 μL DMSO is added to the precipitate. The mixture is stirred magnetically for 1-2 min, resulting in the complete dissolution of the precipitate and the formation of a stable, transparent, and colorless ZnO QD ink. The final ink is transferred into a dry glass vial, closed with a cap, and kept in a refrigerator at -20 °C.

Production and characterization of OPV cells. OPV cells were produced on glass substrates covered with pre-patterned indium tin oxide (ITO). The ITO/glass substrates were cleaned by a multi-step procedure, including (i) sonication in deionized (DI) water, (ii) sonication in acetone, (iii) sonication in 2-propanol (each sonication step performed for 15 min), and (iv) UV-ozone treatment under 253.7-nm irradiation for 15 min. Two layers of ZnO QDs were spin-coated on freshly cleaned glass/ITO substrates. The first layer was spin-coated at 3000 rpm and annealed in air at 200^{o}C for 5 min. Then, the second layer of ZnO QD ink was spin-coated at 3000 rpm, and the resulting film was annealed again at 200^{o}C in the air for 30 min.

An active layer consisting of a mixture of PTQ10 and Y12 (1:1), a mixture of PM6 and L8BO (1:1.2), a mixture of PM6, L8BO, and PC70BM (1:1:0.2) or a quaternary mixture of PM6, L8BO, BTP-eC9 and $PC_{70}BM$ (1:0.663:0.663:0.22) was deposited on ZnO-coated ITO substrates by spin-coating in a nitrogen-filled glove box. In 30 minutes before the spin-coating, respectively 0.50%, 0.25%, and 0.30% of diiodooctane (DIO) were added to PTQ10:Y12, two other PM6-based active layer solutions, and a quaternary mixture. Stock solutions of PTQ10:Y12 in o-xylene and PM6:L8BO, PM6:L8BO:$PC_{70}BM$, as well as PM6, L8BO, BTP-eC9, and $PC_{70}BM$ in chloroform were used. In the particular case of quaternary mixture of PM6, L8BO, BTP-eC9 and $PC_{70}BM$, 25 μL of active layer solution in chloroform (16.9 mg/mL, containing 0.30 w.% octadecyl iodide as an additive) was spin-coated over ZnO at 4200 rpm, left drying for 40 s, and finally annealed in nitrogen at 100 ^{o}C for 10 min.

A hole transport layer (HTL) of molybdenum oxide MoO_x was deposited for the cells with binary and ternary absorbers. In the case of the quaternary absorber, the BM-HTL-1 hole transport material

ink was diluted with ethanol (3:1) was spin-coated at 2500 rpm, and annealed at 100^{o}C for 5 mins. The preparation of the cells was finalized by thermal evaporation of patterned silver contacts with a thickness of ca. 100 nm as a top electrode, using a mask with an opening area of 0.037 mm^2 under 1×10-6 bar, producing six separate identical cells for further characterization.

Reference cells were produced with commercial zinc oxide (Avantama) as an ETL material. In a typical procedure, 60 μL ZnO ink was spin-coated on a cleaned ITO/glass substrate at 3000 rpm, dried for 60 s, and annealed at 200^{o}C for 30 min. The rest of the stack of layers of OPV cells was produced similarly to the above-described procedure.

Characterization of inks and films. Absorption and PL spectra of colloidal inks were registered using a Tecan spectrometer (Tecan, Austria) equipped with a Xenon lamp and a monochromator. Spectral measurements were performed for strongly diluted ZnO QD inks (10 μL per 500 μL EtOH) in cuvettes with an optical path of 0.6 cm. Scanning electron microscopy (SEM) imaging was performed using a JEOL JSM-7610F Schottky field emission scanning electron microscope operating under 15-20 kV acceleration voltage.

Characterization of PV devices. The J-V characteristics were measured using a source measurement unit from Botest. Illumination was provided by a solar simulator (Oriel Sol 1A, from Newport) with AM1.5G spectra at 100 mW cm^{-2} under ambient conditions. A metal mask with an aperture of 3.85-3.90 mm^2 was used to precisely evaluate the photovoltaic performance.

The photodegradation test was performed under illumination with ‘‘white’’ LEDs and metal halide lamps with UV range excluded by cut-off filters. The test was performed in a nitrogen atmosphere (water and oxygen pressure kept under 0.5 ppm) with a home-built characterization setup. The J-V characteristics were probed periodically during the test.

Tables

Table S1. Average PV parameters of the cells with quaternary active layer and ZnO QDs as ETL

Series	[NaOH]/[$ZnCl_2$]	Aging T, °C	Aging time, min	Average size, nm	J_{sc}, mA/cm^2	V_{oc}, mV	FF, %	PCE, %
1	0.6	60	10	**3.9**	25.7	875	74.1	**17.1**
	0.8			**4.0**	26.1	876	75.0	**17.2**
	1.0			**4.2**	26.7	876	75.2	**17.8**
	1.4			**4.6**	27.0	877	76.0	**17.8**
	1.6			**5.0**	26.0	877	74.6	**17.2**
	1.8			**5.2**	25.0	878	72.6	**16.8**
2	1.4	22	10	**3.5**	25.25	873	72.6	**16.1**
		40		**4.0**	26.59	874	75.5	**17.4**
		50		**4.4**	27.13	872	76.1	**18.0**
		55		**4.5**	27.28	874	75.8	**18.1**
		60		**4.6**	27.07	875	75.7	**17.7**
		65		**4.7**	26.67	876	75.4	**17.5**
3	1.4	-	0	**3.7**	25.8	870	74.2	**16.7**
		60	5	**4.4**	26.9	872	76.1	**17.8**
			10	**4.7**	26.8	875	75.4	**17.55**
			15	**5.0**	26.4	873	75.2	**17.36**

The parameters of the synthesis of ZnO QD inks are as follows: EtOH volume – 2.5 mL; antisolvent – 4 mL (composition: toluene/hexane = 1/2), redispersion solvent – 1.5 mL (composition: 20 mL EtOH + 0.02 mL DMSO). *Notes*: The accuracies of average size determination, as well as J_{sc}, V_{oc}, *FF*, and PCE measurements, are 0.1 nm, 0.01 mA/cm^2, 1 mV, 0.1%, and 0.01%, respectively.

Table S2. (Photo-)Electric parameters of the cells with the binary active layer and ZnO ETLs before and after the photodegradation test

ETL	State	J_{sc} (mA/cm^2)	V_{oc} (mV)	FF, %	PCE, %	R_s (Ω/cm^2)	R_{sh} 10^4 (Ω/cm^2)
ZnO QDs	Initial	23.43	845	76.3	15.10	0.9	21
	Aged	21.92	830	70.6	12.84	1.0	8.6
Reference	Initial	23.39	856	75.1	15.07	1.7	1.2
	Aged	20.64	837	64.3	11.11	1.8	0.2

Notes: The accuracies of J_{sc}, V_{oc}, *FF*, PCE, R_s, and R_{sh} measurements are 0.01 mA/cm^2, 1 mV, 0.1%, 0.01%, 0.1 Ω/cm^2, and 0.1 Ω/cm^2, respectively.

Figures

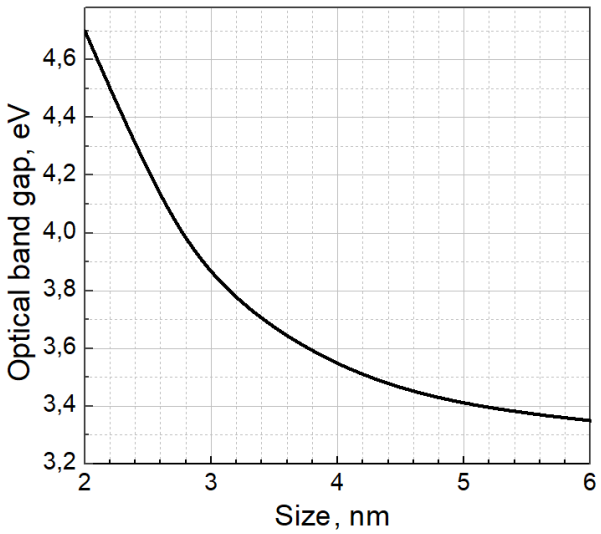

Figure S1. "Size–bandgap" calibration curve for ZnO QDs plotted using the earlier-reported equations (see discussion and references in the main text).

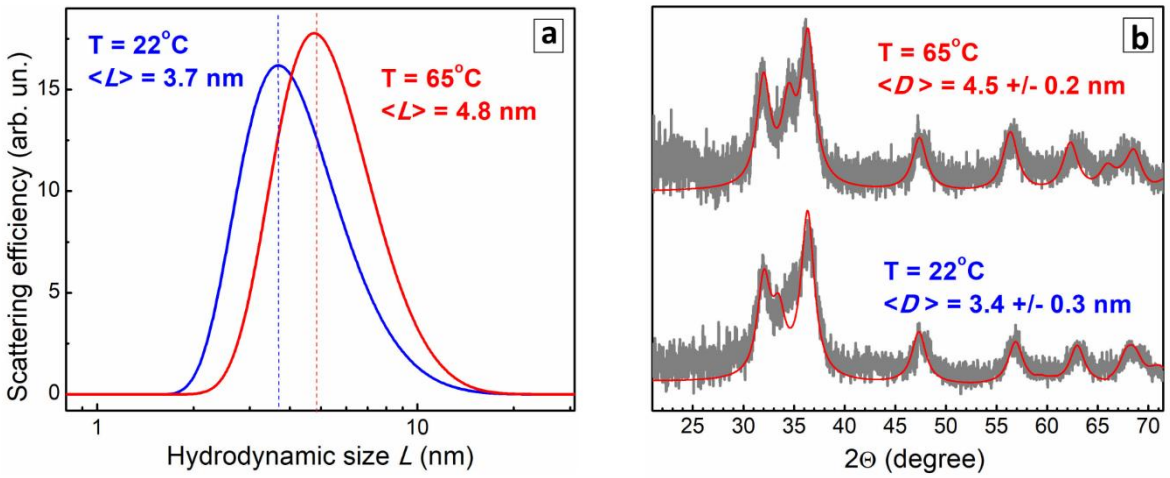

Figure S2. Volumetric distributions of hydrodynamic size (a) and XRD patterns (b) of ZnO QDs produced at 22°C with no annealing and annealed for 10 min at 65 °C.

Dynamic light scattering experiments were carried out using a Zetasizer Nano S (Malvern, UK) at 22°C. Colloids were placed in standard quartz 10.0-mm cuvettes and illuminated by a He-Ne laser at λ = 633 nm. The scattered light was collected at 173° to the laser beam. The average volumetric hydrodynamic size L dHD was determined with an accuracy of 4–5 %. XRD patterns were registered on

thin films of ZnO QDs spin-coated on pre-cleaned glass substrates using a Panalytical X'pert powder diffractometer with filtered Cu K_α radiation (λ = 1.54178 Å) and an X'Celerator solid-state stripe detector in the Bragg-Brentano geometry in an angle range of 2θ = 10-80° with a step rate of 0.05° per min. The XRD patterns were subjected to a Rietveld refinement with MAUD software (version 2.99) using a structural CIF file of hexagonal ZnO from the Crystallography Open Database, COD ID 2300450.

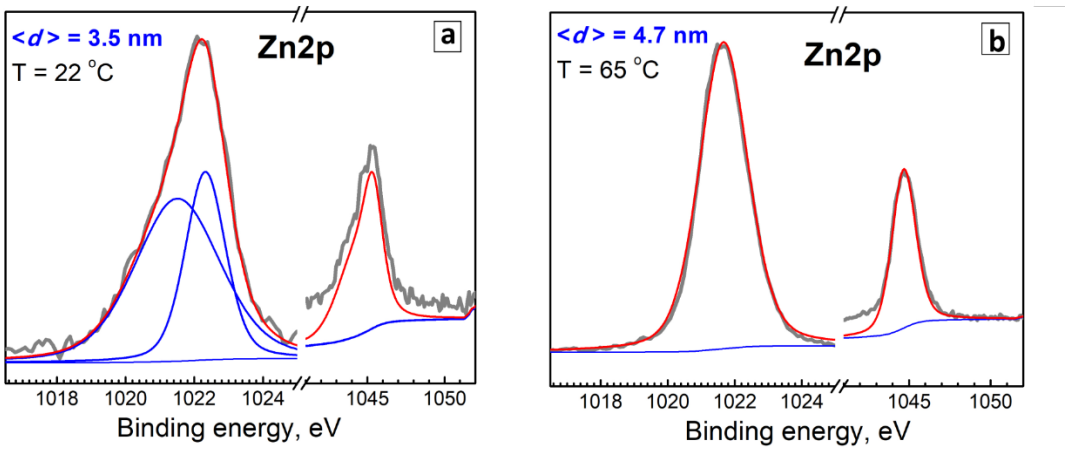

Figure S3. High-resolution X-ray photoelectron (XPS) spectra of Zn 2p series for ZnO QDs produced with no annealing at 22 °C and after annealing at 60 °C for 10 min. Gray lines correspond to experimental data, blue lines represent fittings with Gauss profiles, and red lines show total fitting curves.

XPS measurements were performed with an ESCALAB 250Xi X-ray Photoelectron Spectrometer Microprobe (Thermo Scientific) equipped with a monochromatic Al K_α (1486.68 eV) X-ray source. A pass energy of 20 eV was used for high-resolution core-level spectra, providing a spectral resolution of 0.5 eV. The linearity of the energy scale was calibrated by the positions of the Fermi edge at 0.00 ± 0.05 eV, Au4f7/2 at 83.95 eV, Ag3d5/2 at 368.20 eV, and Cu2p3/2 at 932.60 eV measured on in situ cleaned metal surfaces. To prevent charging, the samples were measured by applying a built-in charge compensation system. The authors thank Prof. Dietrich R.T. Zahn and Dr. Volodymyr Dzhagan (Chemnitz University of Technology, Semiconductor Physics) for their assistance in the acquisition of the X-ray photoelectron spectra.

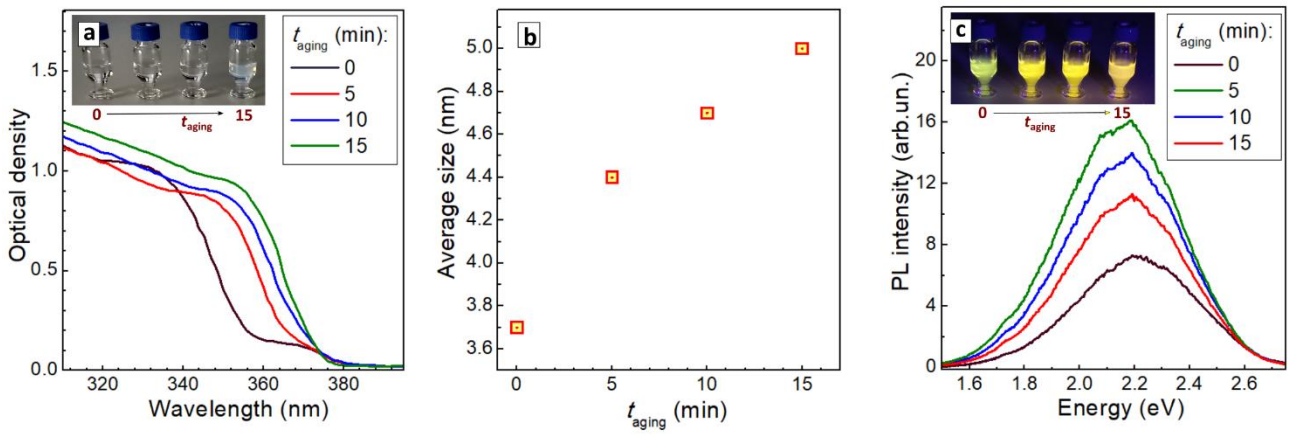

Figure S4. (a,c) Absorption (a) and PL (c) spectra of colloidal ZnO QD inks produced at different aging durations and fixed aging temperature of 60°C and [NaOH]/[$ZnAc_2$] =1.4; inserts show photographs of ZnO QD inks under natural (a) and UV (c) illumination; (b) Average size of ZnO QDs as a function of the aging duration. See Table S1 for more details.

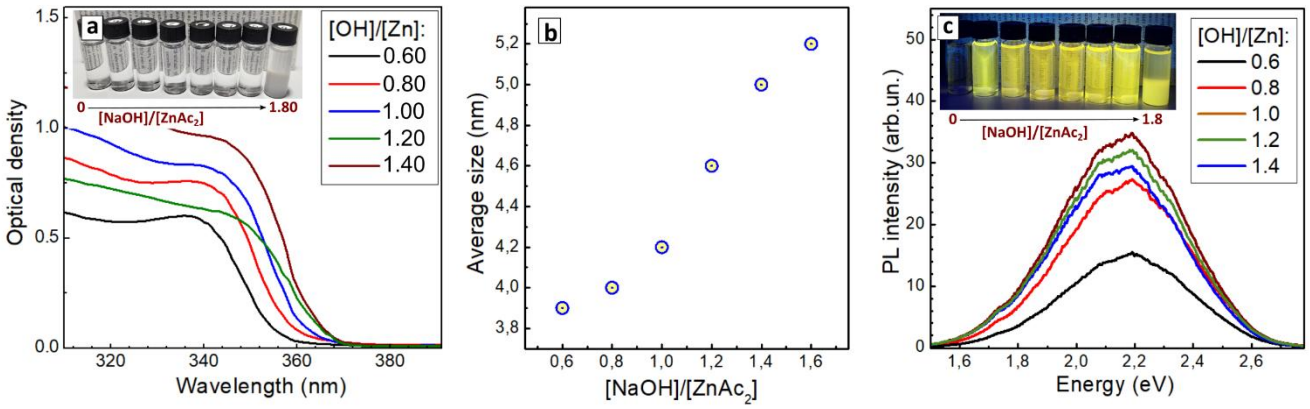

Figure S5. (a,c) Absorption (a) and PL (c) spectra of colloidal ZnO QD inks produced at different [NaOH]/[$ZnAc_2$] ratios and fixed aging temperature of 60°C and aging duration of 10 min; inserts show photographs of ZnO QD inks under natural (a) and UV (c) illumination; (b) Average size of ZnO QDs as a function of the [NaOH]/[$ZnAc_2$] ratio. See Table S1 for more details.

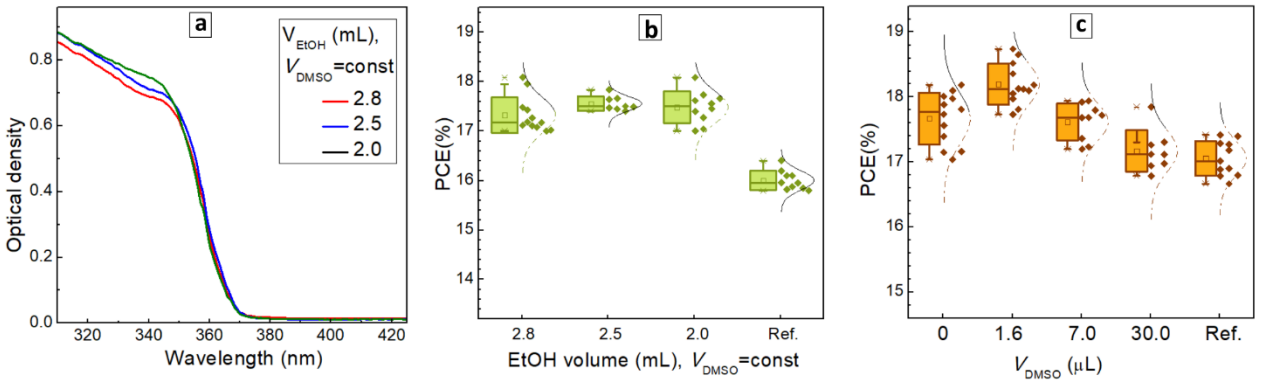

Figure S6. Effect of the DMSO volume used for QD synthesis (a,b) and redispersion (c) on their absorption spectra (a) performance as ETL in comparison with the reference ZnO (b,c).

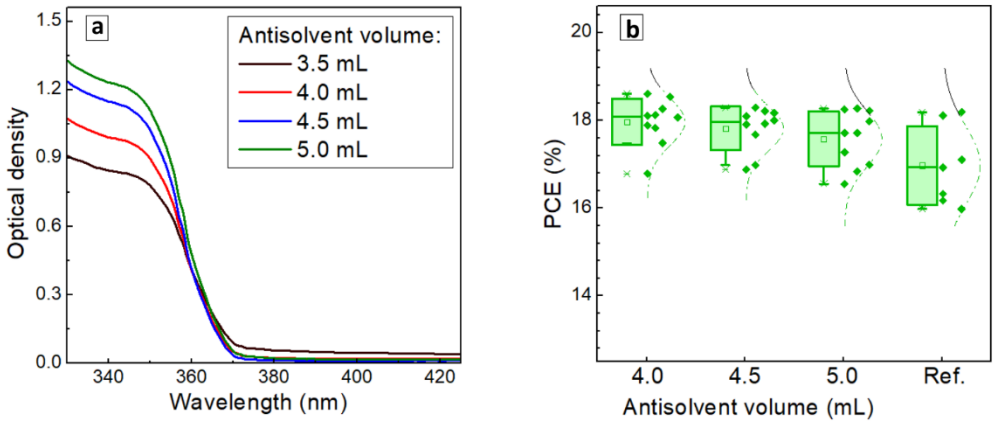

Figure S7. Effect of the antisolvent volume on the absorption spectrum (a) and PV performance of ZnO QDs in comparison with the reference ZnO.

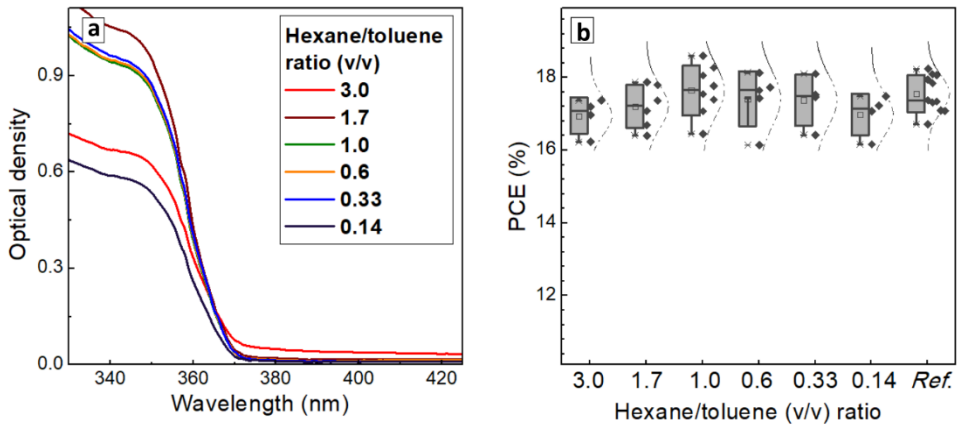

Figure S8. Effect of the antisolvent composition (volumetric toluene-to-hexane ratio) on the absorption spectrum (a) and PV performance of ZnO QDs in comparison with the reference ZnO (Refs.).

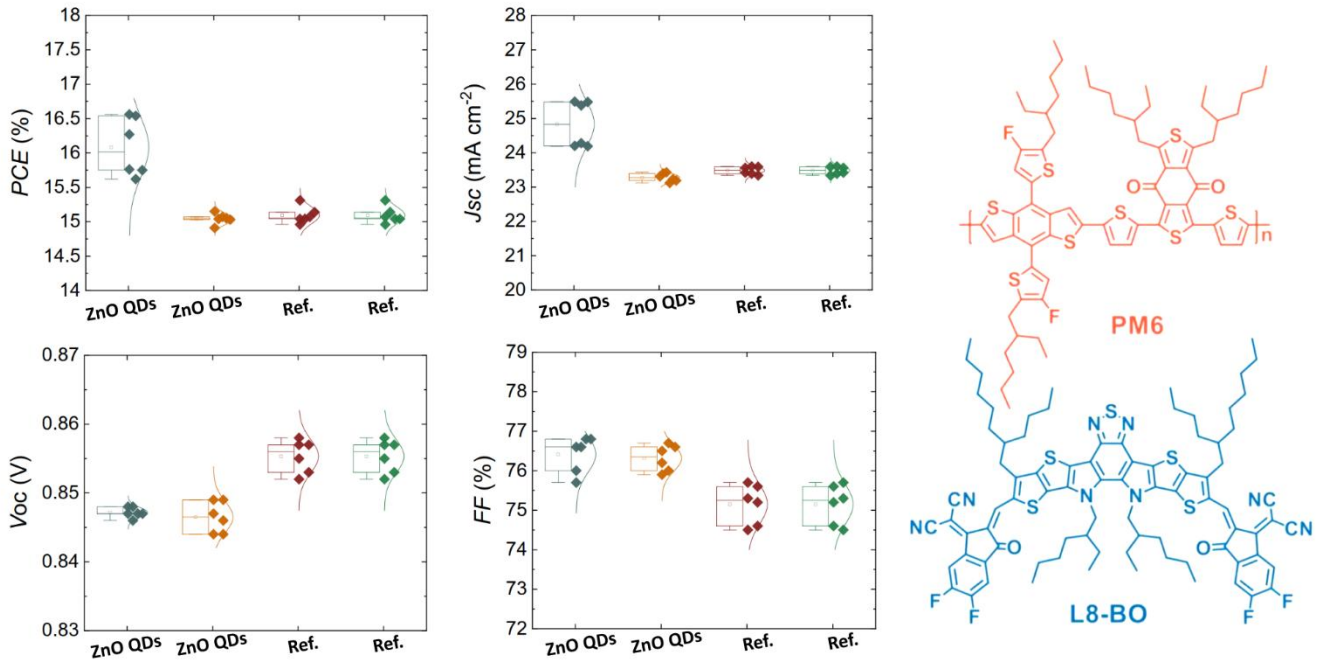

Figure S9. Distributions of PCE, J_{sc}, V_{oc}, and FF for the cells with the binary PM6:L8-BO active layer and ETL produced from reference ZnO and ZnO QDs (two sets of measurements each). The right panel shows the chemical structures of the active layer components.

Abbreviations:

PM6 - Poly[(2,6-(4,8-bis(5-(2-ethylhexyl-3-fluoro)thiophen-2-yl)-benzo[1,2-b:4,5-b']dithiophene))-alt-(5,5-(1',3'-di-2-thienyl-5',7'-bis(2-ethylhexyl)benzo[1',2'-c:4',5'-c']dithiophene-4,8-dione)], brutto-formula: $(C_{68}H_{76}F_2O_2S_8)_n$

L8BO - 2,2'-((2Z,2'Z)-((3,9-bis(2-butyloctyl)-12,13-bis(2-ethylhexyl)-12,13 dihydro[1,2,5]thiadiazolo[3,4-e]thieno[2'',3'':4',5']thieno[2',3':4,5]pyrrolo[3,2-g]thieno[2',3':4,5]thieno[3,2-b]indole-2,10-diyl)bis(methanylylidene))bis(5,6-difluoro-3-oxo-2,3-dihydro-1H-indene-2,1-diylidene))dimalononitrile, brutto-formula: $C_{84}H_{90}F_4N_8O_2S_5$

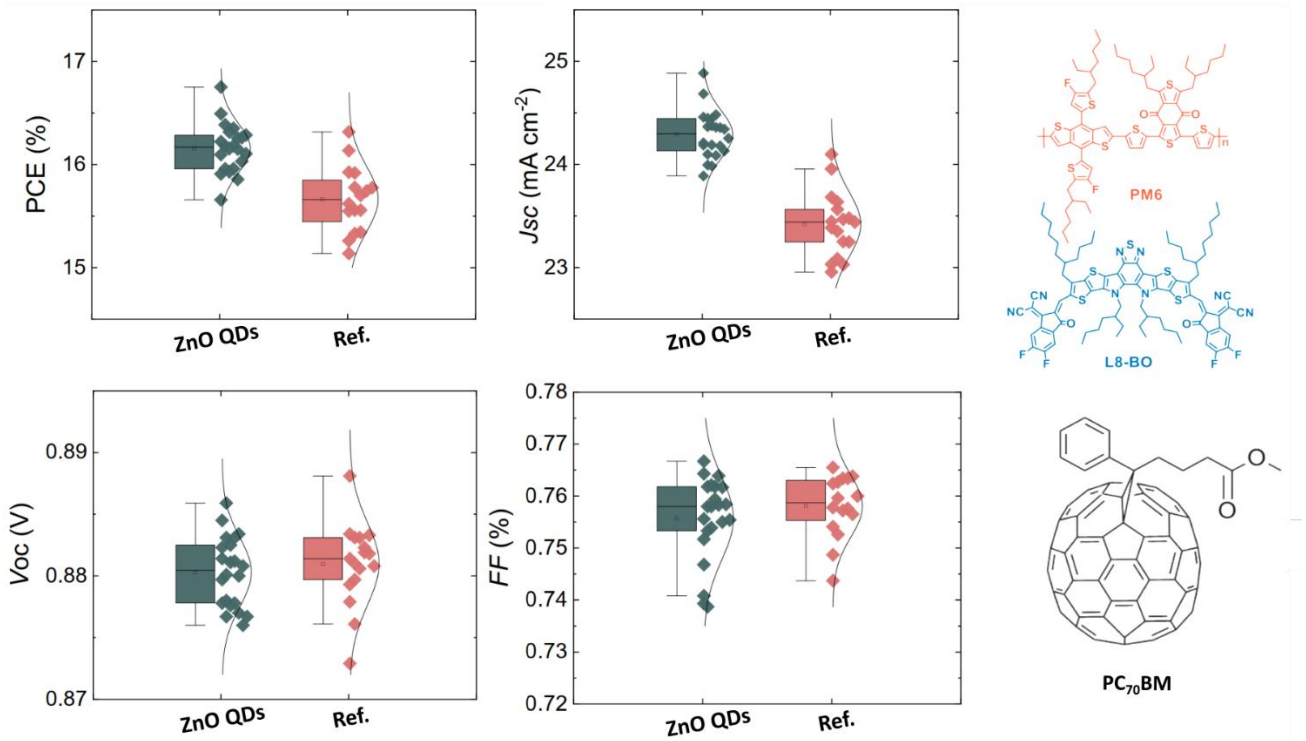

Figure S10. Distributions of PCE, J_{sc}, V_{oc}, and FF for the cells with the ternary PM6:L8-BO:$PC_{70}BM$ active layer and ETL produced from reference ZnO and ZnO QDs. The right panel shows the chemical structures of the active layer components.

Abbreviations:

$PC_{70}BM$ - [6,6]-Phenyl-C_{71}-butyric acid methyl ester, brutto-formula: $C_{82}H_{14}O_2$

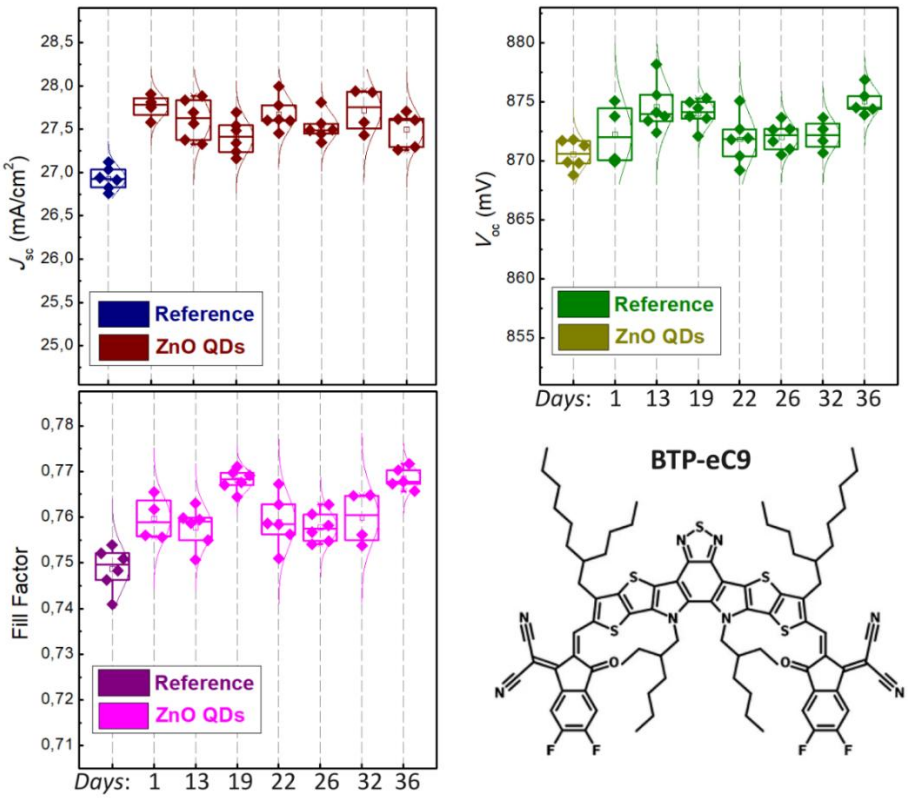

Figure S11. Distributions of J_{sc}, V_{oc}, and FF for the cells with the quaternary PM6:L8-BO:$PC_{70}BM$:BTP-eC9 active layer and ETL produced from reference ZnO and ZnO QDs stored at -20°C for different periods (in days). The right lower panel shows the chemical structures of the active layer components.

Abbreviations:

BTP-eC9 - 2,2'- [[12,13-Bis(2-butyloctyl)-12,13-dihydro-3,9-dinonylbisthieno[2'',3'':4',5']thieno[2',3':4,5]pyrrolo[3,2-e:2',3'-g][2,1,3]benzothiadiazole-2,10-diyl]bis[methylidyne(5,6-chloro-3-oxo-1H-indene-2,1(3H)-diylidene)]]bis[propanedinitrile], brutto-formula: $C_{86}H_{94}Cl_4N_8O_2S_5$

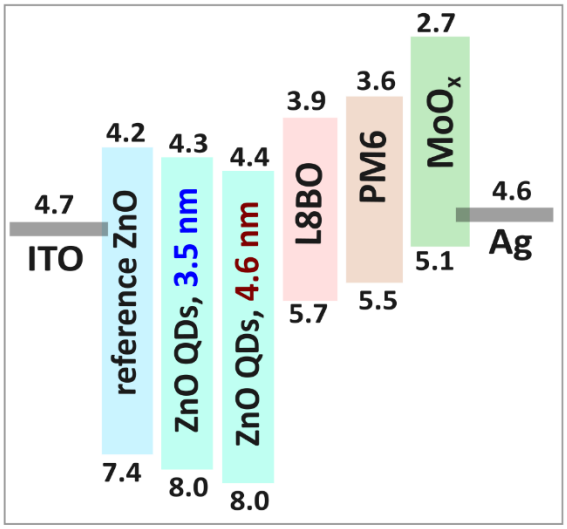

Figure S12. Energy diagram of an exemplary solar cell based on different ITO/ZnO ETLs (reference ZnO, ZnO QDs with the average QD size of 3.5 nm produced with no annealing, and ZnO QDs with the average QD size of 4.6 nm produced by the annealing at 60 °C for 10 min), PM6:L8BO bulk heterojunction absorber, MoO_x HTL, and Ag back electrode. The numerical values for absorber components, electrodes, and MoO_x are taken from [S1-S3].

References

[S1]. H.N. Tran, S. Park, F.T. Adhi Wibowo, N.V. Krishna, J.H. Kang, J.H. Seo, H. Nguyen-Phu, S.Y. Jang, S. Cho, Adv. Sci. 2020, 7, 2002395.

[S2]. 41. J. Bertrandie, J. Han, C.S.P. De Castro, E. Yengel, J. Gorenflot, T. Anthopoulos, F. Laquai, A. Sharma, D. Baran, Adv. Mater. 2022, 34, 2202575.

[S3]. C. Zhang, J. Li, W. Deng, J. Dai, J. Yu, G. Lu, H. Hu, K. Wang, Adv. Func. Mater. 2023, 33, 2301108.

The work functions of ZnO ETLs were evaluated using Kelvin probe measurements on films deposited on ITO in conditions identical to those used for the solar cell preparation using a scanning Kelvin probe system SKP5050 (UK). Each work function measurement was performed for three different samples, yielding an accuracy of ±0.1 eV.

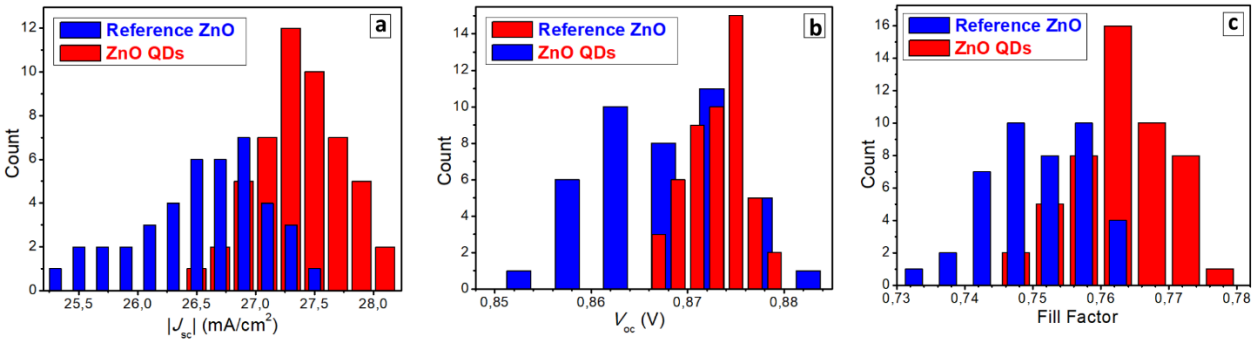

Figure S13. Statistical distributions of J_{sc} (a), V_{oc} (b), and FF (c) values collected for solar cells with the quaternary active layer and ETL = ZnO QDs (red bars) and ETL = reference ZnO (blue bars).

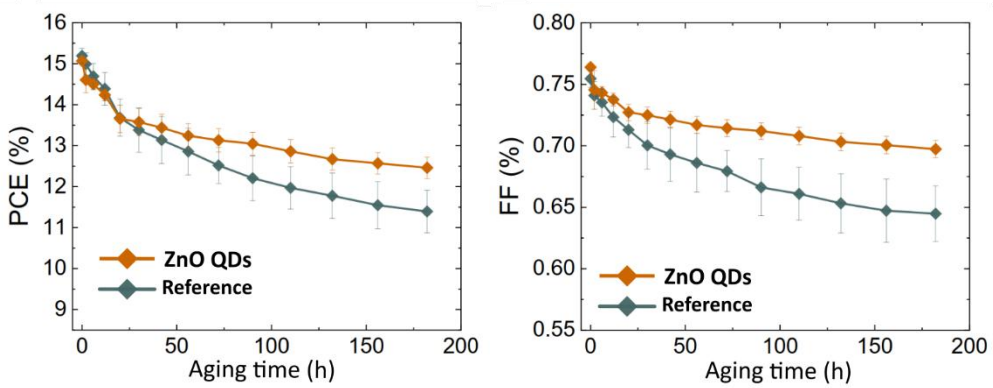

Figure S14. Evolution of actual PCE and FF of solar cells with the binary active layer and ZnO ETLs during the photodegradation test.

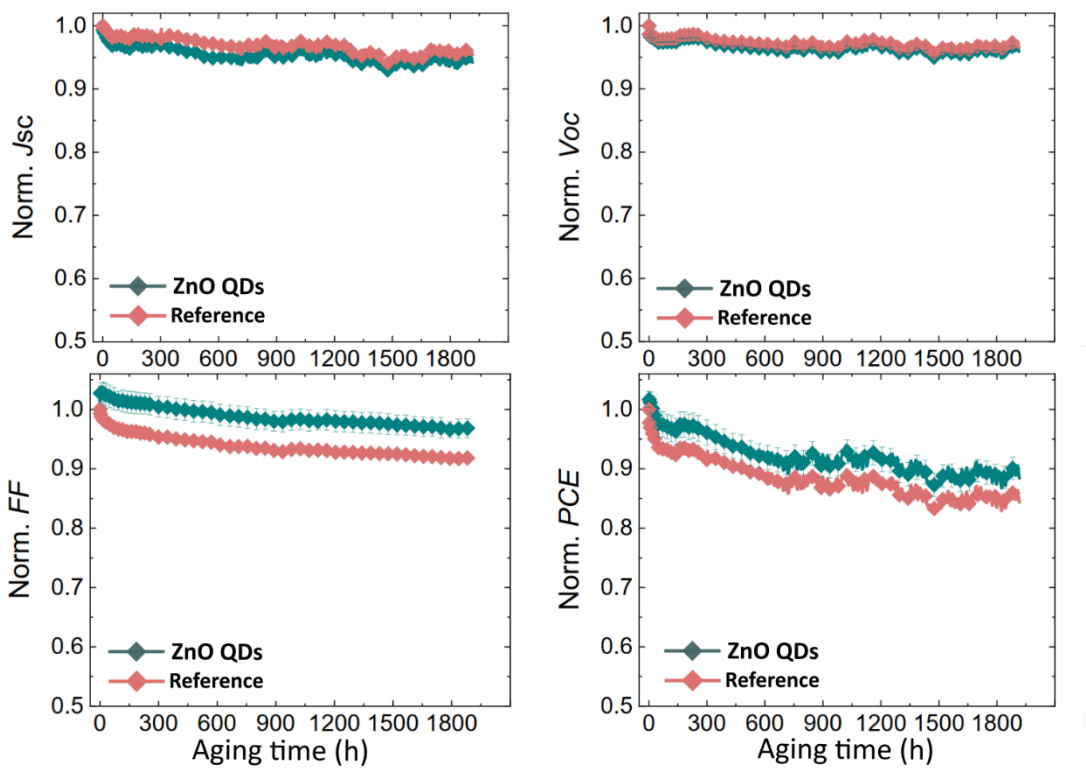

Figure S15. Evolution of normalized J_{sc}, V_{oc}, FF, and PCE of solar cells with the ternary active layer and ZnO ETLs (QDs and reference) during the photodegradation test.

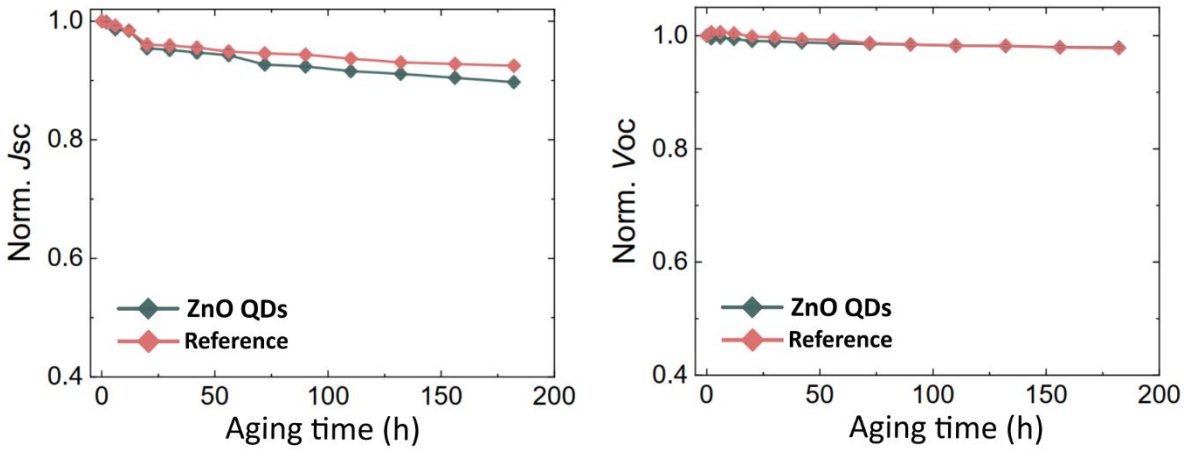

Figure S16. Evolution of normalized J_{sc} and V_{oc} of solar cells with the binary active layer and ZnO ETLs during the photodegradation test.

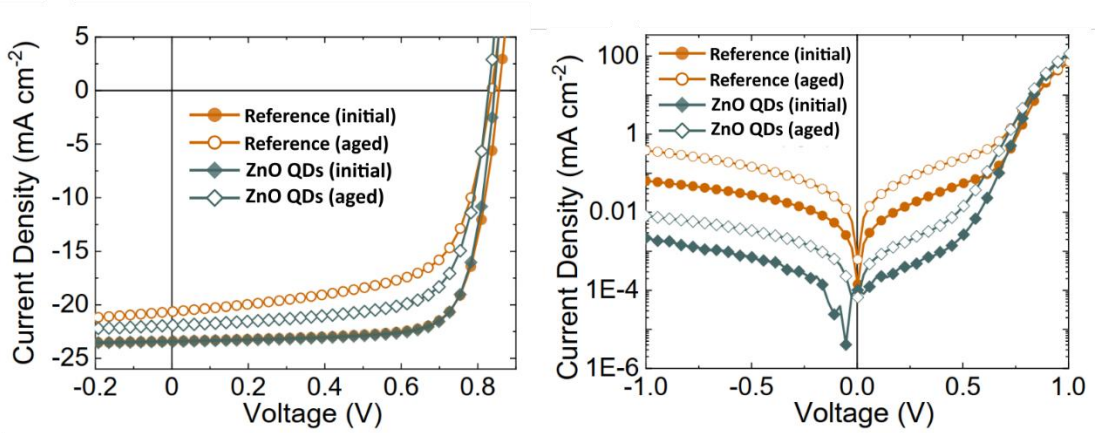

Figure S17. Current-voltage characteristics of solar cells with the binary active layer and ZnO ETLs (QDs and reference) before (initial) and after (aged) the photodegradation test. Left figure: measurements under 1-Sun illumination, right figure: in the dark.

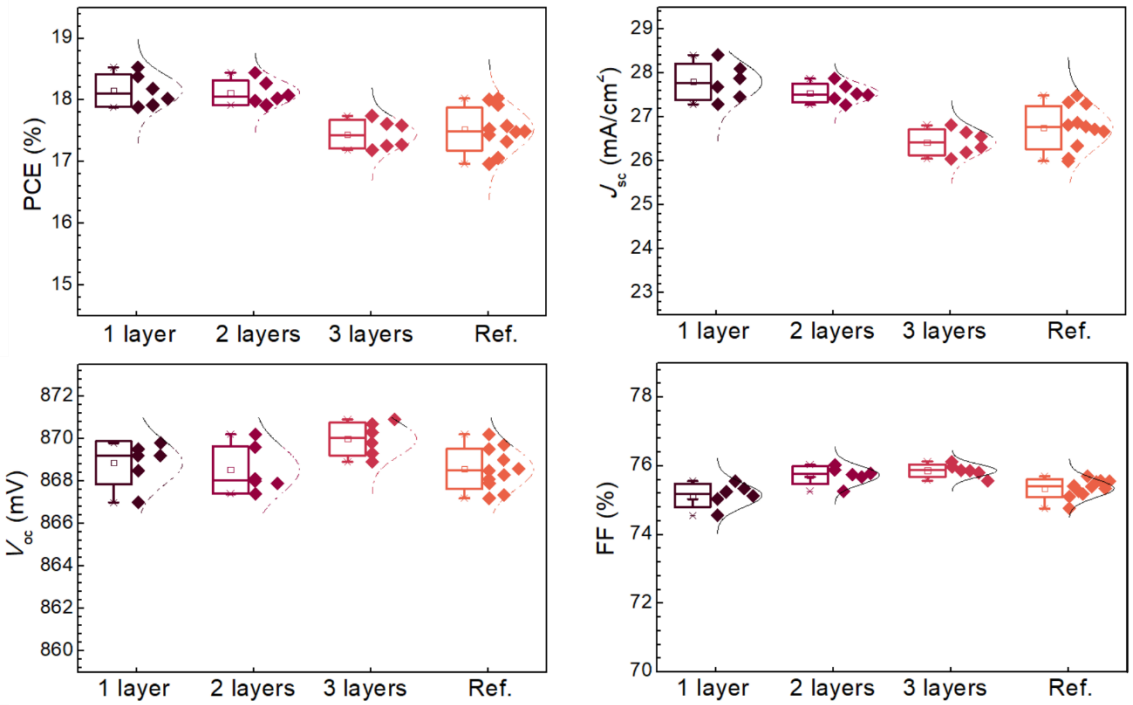

Figure S18. Effect of the number of layers (1-3) of ZnO QDs on their performance as ETL in comparison with the reference ZnO (Ref.).

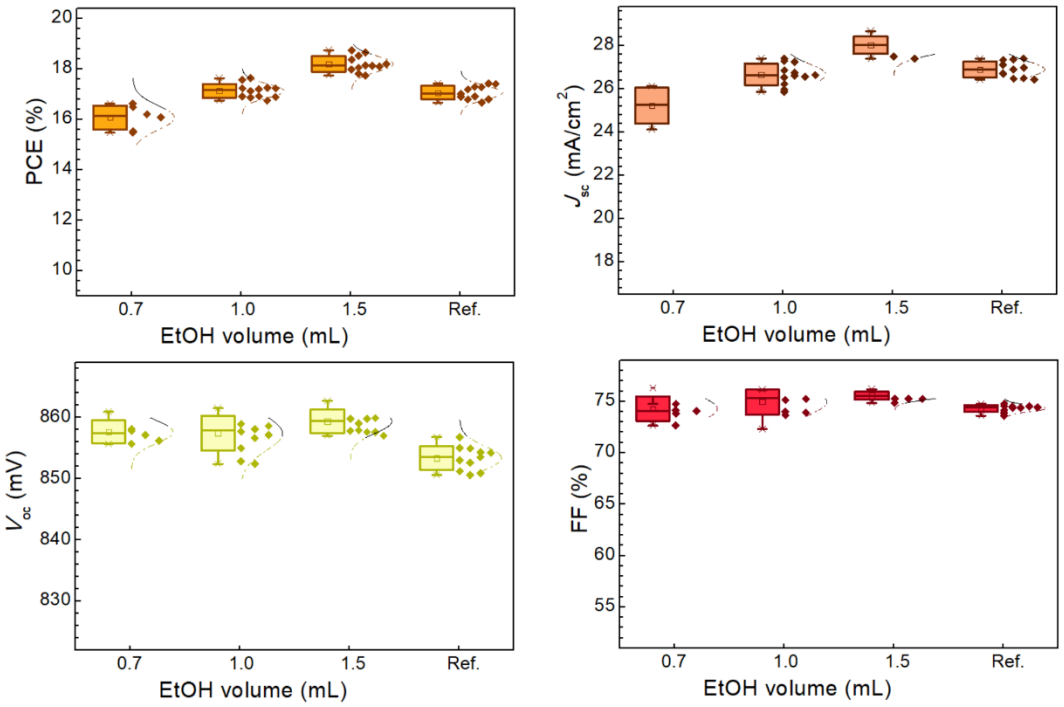

Figure S19. Effect of the EtOH volume used for QD redispersion (that is, the actual ZnO concentration) on their performance as ETL in comparison with the reference ZnO (Ref.).

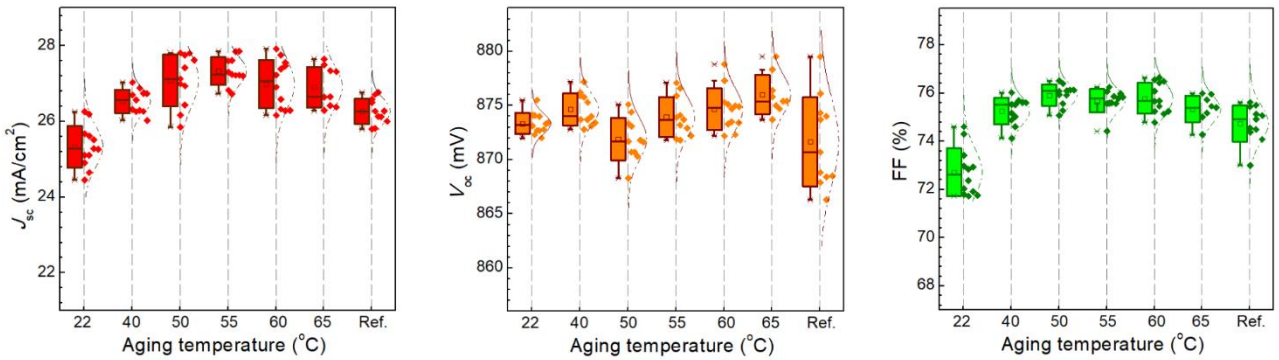

Figure S20. PV parameters (J_{sc}, V_{oc}, and FF) of the solar cells with the quaternary active layer, ZnO reference EL (Ref.), and ZnO QD ETLs produced at different aging temperatures of the ZnO QD inks with fixed aging duration (10 min) and [NaOH]/[$ZnAc_2$] =1.4. More details are in Table S1.

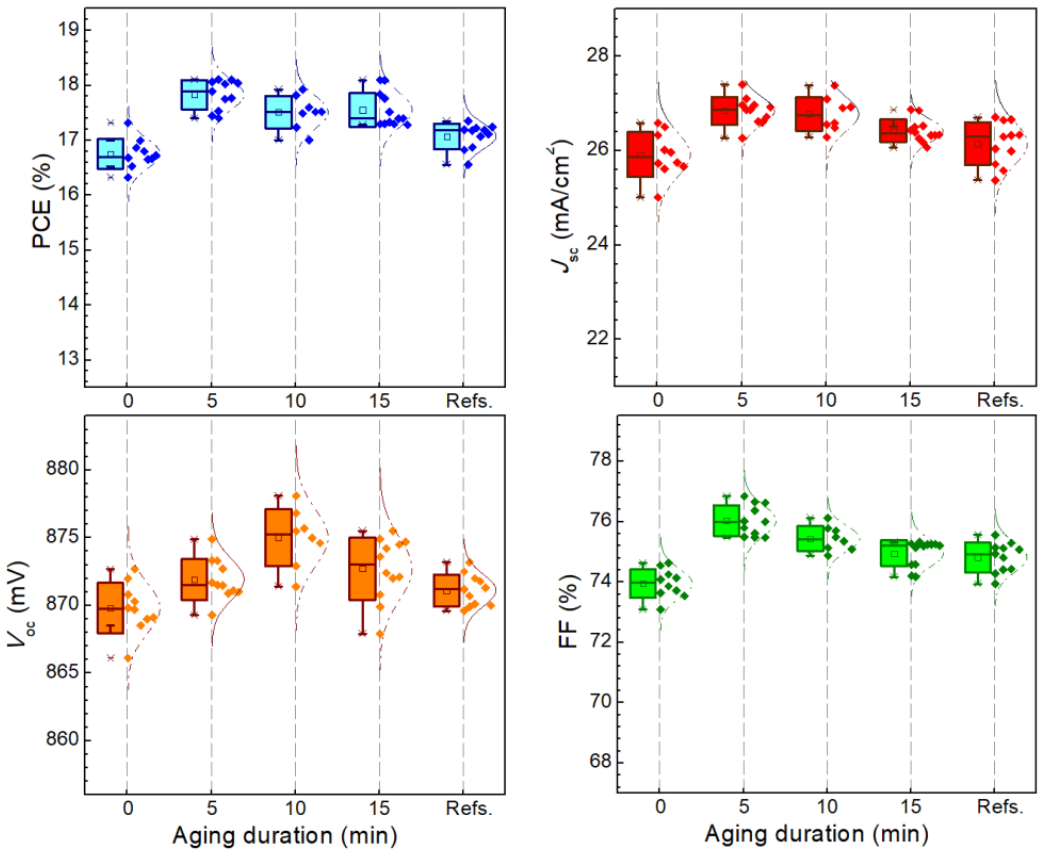

Figure S21. PV parameters (PCE, J_{sc}, V_{oc}, and FF) of the solar cells with the quaternary active layer, ZnO reference EL (Ref.), and ZnO QD ETLs produced at different aging duration the ZnO QD inks with fixed aging temperature (60^{o}C) and [NaOH]/[$ZnAc_2$] = 1.4. More details are in Table S1.

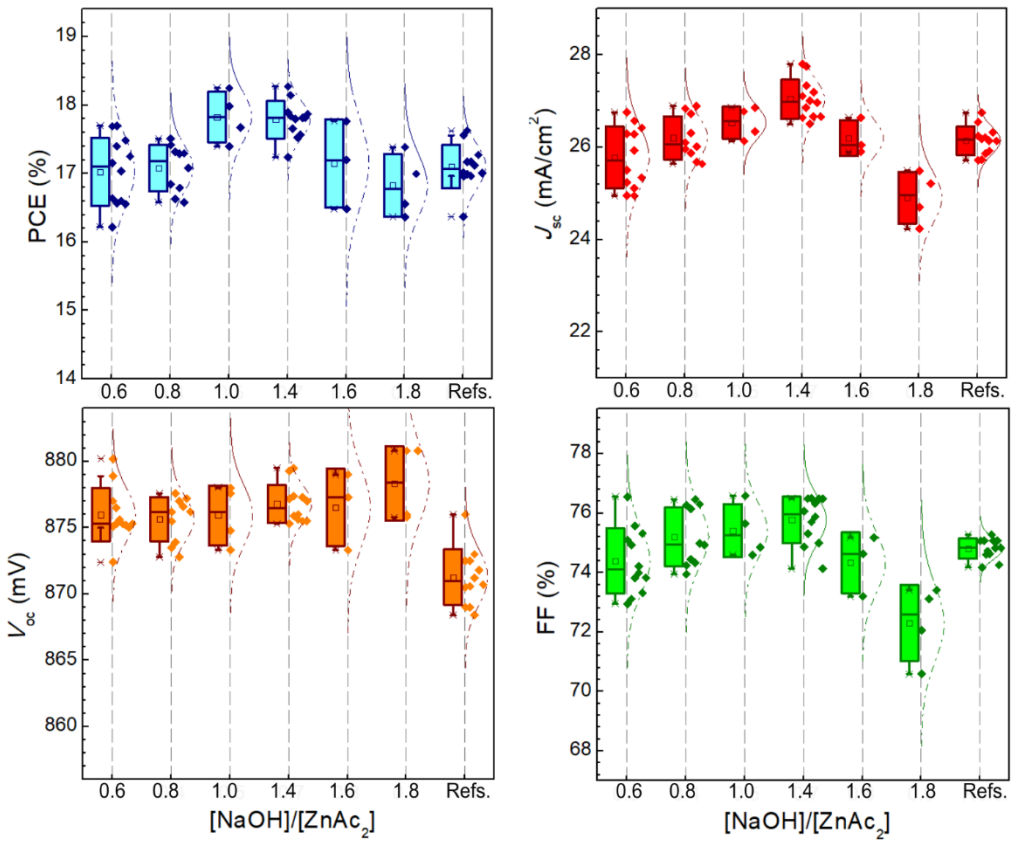

Figure S22. PV parameters (PCE, J_{sc}, V_{oc}, and FF) of the solar cells with the quaternary active layer, ZnO reference EL (Ref.), and ZnO QD ETLs produced at different [NaOH]/[$ZnAc_2$] ratios with fixed aging temperature (60°C) and aging duration (10 min). More details are in Table S1.

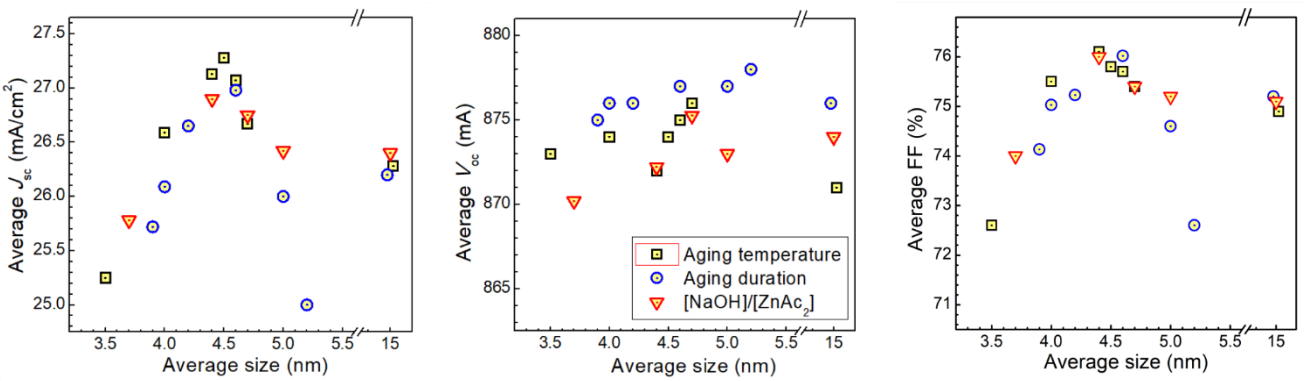

Figure S23. Dependences of average J_{sc}, V_{oc}, and FF of the solar cells with the quaternary active layer on the average size of ZnO QDs in the ETL layer. Data was collected for three size-selected series on aging temperature (squares), aging duration (triangles), and [NaOH]/[$ZnAc_2$] ratio (circles). See Table S3 for more details.